JOURNAL OF MATERIALS SCIENCE 13 (1978) 2418–2428

The structural characteristics of radiation damage produced by high energy (2.7 MeV) ion implantation in GaAs

G. H. NARAYANAN, W. G. SPITZER
Department of Materials Science, University of Southern California, Los Angeles, California 90007, USA

The radiation damage induced by the implantation of 2.7 MeV P^+ and N^+ ions with a dose of 6.4×10^{16} ions cm^{-3} into GaAs at room temperature has been studied by transmission electron microscopy. The as-implanted material was found to consist of a buried amorphous layer which was sandwiched between a heavily damaged but crystalline cover layer exhibiting a high density of black dot defects, microtwins and dislocation loops and a less damaged substrate region. Post-implantation annealing of the specimens at 250° C for 6 h resulted in the recrystallization of the amorphous and cover layers by random nucleation of grains producing a polycrystalline region on the single crystal substrate. However, a second stage annealing of these samples at 400° C for 2 h caused an epitaxial regrowth of the implanted layer on the undamaged substrate producing single crystal regions which were heavily twinned on all {1 1 1} planes. The results of the present microstructural analyses have been compared with the previous infra-red reflectivity studies on identically implanted GaAs samples to determine the effects of structural changes on the dielectric properties. The two studies are found to be in reasonable agreement. The present results are also compared with those from previous lower energy–lower dose implantations.

1. Introduction

Ion implantation of dopant atoms has now been successfully employed to produce both p-type and n-type layers on GaAs substrates. High energy implantation, however, introduces considerable damage to the host lattice, the extent of which is determined by the mass, energy and dose of the implanted ions, the mass of the target atoms, as well as the temperature of the target. In extreme cases, the atomic disorder in the implanted region can be sufficiently great as to cause crystalline-to-amorphous transitions to occur. Any impurity conduction effect arising from the electrical (doping) characteristics of the implanted ion is generally completely masked by the damage. Therefore the damage must be annealed out by appropriate post-implantation heat treatment which will reduce the residual defects to a level where carrier mobilities and lifetimes are usefully large and the implanted ions will be incorporated into electrically active sites in the crystal lattice. Thus, it is of great interest to study the nature of implantation-induced damage as a function of implantation conditions and the recovery of the damage during post-implantation annealing.

In some recent studies of ion-implanted GaAs Kachare *et al.* [1–3] demonstrated that the implantation-induced changes in optical properties can be used as a tool to characterize the extent of the damage produced by the implantation. More specifically, it has been shown that the near infrared refractive index of GaAs can be substantially increased by the lattice damage caused by large dose ion-implantation and that these changes in refractive indices exhibit a depth distribution related to that of the damage concentration [2, 3]. The room temperature near infra-red reflection and transmission were measured over a

© 1978 Chapman and Hall Ltd. Printed in Great Britain.

wide range of photon energies on GaAs implanted at 2.7 MeV P^+ ions with a fluence of 6.4×10^{16} cm^{-2}, and these measurements revealed interference fringe patterns which were strongly amplitude modulated. It has been shown by Kachare *et al.* [2, 3] that the reflection fringes could be analysed in terms of a simple model in which the implanted material was approximated by a heavily damaged and buried layer sandwiched between a partially-absorbing cover layer and a non-absorbing substrate. A detailed analysis of the measured fringe patterns by using a curve fitting procedure indicated that the effective layer thicknesses were comparable to those predicted by the projected range of the ions and width of the Gaussian ion distribution. Annealing of the specimens at $\lesssim 400°$ C resulted in a reduction in implantation-induced changes in refractive index, with the buried and cover layers becoming optically essentially the same, indicating the removal of the damage during annealing. The implant layer thickness, on the other hand, remained unchanged. The general conclusions of this study was that the implantation-induced damage in GaAs does not primarily anneal out by an epitaxial regrowth process as has been observed for heavily implanted Si, at least in the temperature range investigated.

Although optical measurements of the type described above give some idea about the extent of the damage no precise information regarding the structural characteristics of the damage can be deduced. In the present investigation, therefore, transmission electron microscopy was used to study the lattice damage induced by the implantation of 2.7 MeV P^+ and N^+ ions in the GaAs samples. These samples are the same or identical to those which were previously studied by the optical properties measurement techniques. The microstructural changes accompanying the post-implantation annealing treatments at 400° C and below have been followed to establish the processes involved in the elimination of the implantation-induced damage.

The results indicate that the ion implanted region in these GaAs samples consists of an amorphous layer buried below a heavily damaged crystalline cover layer, thus confirming the layer model proposed by Kachare *et al.* [2, 3]. The removal of the damage during post-implantation annealing at 250° C is shown to occur by the recrystallization of both the buried amorphous and crystalline cover layers which results in the formation of a polycrystalline surface layer. A different annealing mechanism is shown to operate during a second stage annealing at a higher temperature, that is 400° C, by which a regrowth of the damaged layer occurs epitaxially on the substrate as has been observed for heavily implanted Si having the same orientation [4].

2. Experimental procedure

The details of the procedure for ion implantation of GaAs used in this study are essentially those described in previous papers [2] and therefore only a brief description will be included here. Wafers of GaAs cut from undoped ingots were initially mechanically polished to 0.5 mm thickness. One surface of the wafer was then chemically polished to remove the surface damage. The polished surface was implanted with $^{31}P^+$ $^{14}N^+$ ions by using the Van de Graff accelerator at the Rome Air Developmental Center, Hanscom Air Force Base. During implantation the wafers were mounted on a water-cooled holder with a thin layer of vacuum grease between the lapped specimen surface and the holder to improve the thermal contact. One wafer, having ⟨1 0 0⟩ orientation was implanted with $^{31}P^+$ ions having an energy of 2.7 MeV at a dose rate of 1.3×10^{12} ions cm^{-2} sec^{-1} to give a total dose of 6.4×10^{16} ions cm^{-2}. A second wafer having a ⟨1 1 0⟩ orientation was implanted with 3.0 MeV $^{14}N^+$ ions and a total dose of 2.0×10^{17} ions cm^{-2}. After the implantation the samples were cleaned with a 50–50 toluene–methanol mixture and any residual carbon deposit removed by 15 to 30 min of cold oxygen plasma treatment. Post-implantation annealing of the samples was carried out in cleaned, evacuated sealed quartz ampoules, at 250° C and 400° C. Two different annealing procedures were used: a single step annealing where the samples were heated directly to 250 or 400° C and a double step annealing where the samples which were initially annealed at 250° C for 6 h were subsequently heated to 400° C for 2 h.

From the as-implanted and the annealed GaAs, specimens 3 mm × 3 mm in size suitable for transmission electron microscopy were cut with a wire saw. It has been shown from previous studies [2, 3] that the region of maximum lattice damage in 2.7 MeV P-implanted samples occurs as a buried layer of ~ 0.3 μm in thickness beneath a cover layer of ~ 2 to 2.3 μm in thickness. Therefore a two stage thinning procedure involving

both ion beam milling and chemical jet polishing steps was used to insure that the buried layer was included in the thin foil specimen. Ion beam milling was initially employed to remove in a controlled manner a layer $\sim 2\,\mu m$ in thickness from the implanted side. Final thinning to electron transparency was accomplished by chemical jet polishing from the substrate side. All specimens were examined in a Hitachi HU-125 transmission electron microscope operated at 125 kV with the implanted side facing the incident electron beam.

3. Results

3.1. As-implanted material

Fig. 1a shows a typical electron diffraction pattern obtained from the heavily damaged region of a GaAs specimen implanted with $^{31}P^+$ ions having an incident energy of 2.7 MeV and a total dose of 6.4×10^{16} ions cm^{-2}. This heavily damaged region occurs at a depth of $2\,\mu m$ below the original surface which roughly corresponds to the position of the peak in the depth distribution of the implanted species in the specimen. The pattern in Fig. 1a is composed of three diffuse rings or halos surrounding the central spot, and is characteristic of those produced by amorphous films. Thus it is quite evident that implantation of higher energy P^+ ions in large doses has driven GaAs in this region into an amorphous state.

The electron transparent regions of the specimen had a tapered cross-section as shown in Fig. 1b so that the foil thickness increased slowly with distance from the jet-etched hole. The diffraction pattern shown in Fig. 1a was obtained from the thinnest regions of the foil, which consisted only of the amorphous layer. The patterns taken from the adjacent thicker areas of the foil revealed, in addition, the presence of diffraction spots arising from crystalline GaAs which were super-imposed on the diffused rings from the amorphous layer. An example is shown in Fig. 1c. It can be noticed that the strong diffraction spots are also circled by diffuse rings. This is clearly a double diffraction effect whereby the strong diffracted beams originating from the crystalline region act as new sources for further diffraction from the amorphous region. Since in the present study all the specimens were examined in the microscope with the implanted side facing the incident electron beam, the above observation clearly implies that overlying the amorphous region there exists a relatively less damaged crystalline layer. A similar observation was reported by Sealy [5] on ⟨1 1 0⟩ oriented GaAs implanted at room temperature with 2.5×10^{15} Te^+ ions cm^{-2} at 150 keV where

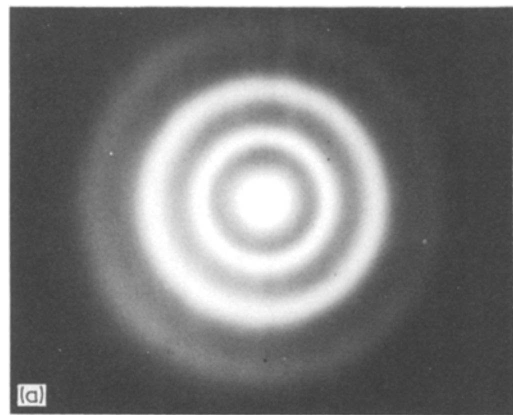

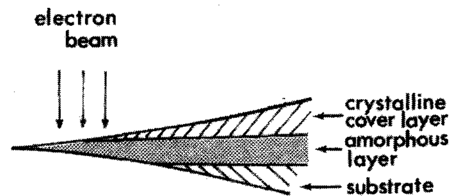

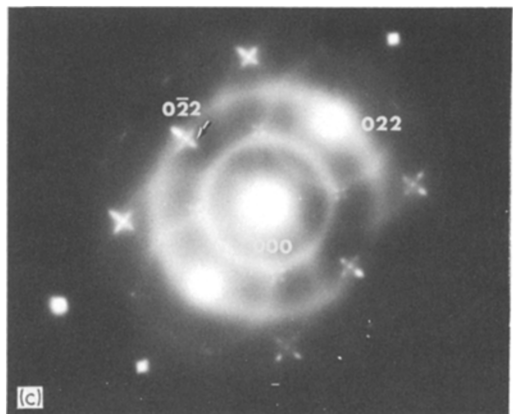

Figure 1 (a) A transmission electron diffraction pattern obtained from the heavily damaged region $\sim 2\,\mu m$ below the surface of a 2.7 MeV P^+ implanted GaAs specimen. (b) A schematic diagram of the cross-section of a tapered thin foil specimen showing the layered structure produced by 2.7 MeV P^+ implantation. (c) An electron diffraction pattern obtained from the thicker region of the foil showing the presence of a heavily twinned crystalline cover layer above the amorphous layer. (d) A schematic diagram illustrating the origin of the elliptical satellite reflections in Fig. 1c in terms of the intersections of ⟨1 1 1⟩ reciprocal lattice spikes with the sphere of reflection.

the implantation produced gross lattice damage in the form of a continuous amorphous layer sandwiched between the substrate and a crystalline surface layer.

The spot pattern shown in Fig. 1c can be indexed as that due to GaAs, which is tilted off the exact ⟨1 0 0⟩ orientation about a ⟨0 2 2⟩ axis. An additional feature of this pattern is the presence of four satellite spots around each of the matrix reflections that lie on either side of the tilt axis. These satellite spots which are elliptical in shape are displaced from the matrix reflection along the ⟨0 2 2⟩ directions. Tilting the specimen to exact ⟨1 0 0⟩ orientation caused these satellite spots to disappear, indicating that they do not lie in the {1 0 0} reciprocal lattice plane. Pashley and Stowell [6] have shown that the reciprocal lattice points due to twins occurring on all the {1 1 1} planes of an f c c matrix either coincide with the matrix spots or are displaced from the matrix spots by vectors of $\pm 1/3$ ⟨1 1 1⟩. As a consequence of the equivalence of the f c c and sphalerite lattices, the above analysis is also applicable to the present case. In addition, if the twins are in the form of thin platelets (which is the case with microtwins), the twin reciprocal spots will be streaked along the ⟨1 1 1⟩ direction. These ⟨1 1 1⟩ streaks will intersect the {1 0 0} matrix reciprocal lattice plane obliquely. The origin of the elliptical satellite spots which are displaced along the ⟨0 1 1⟩ directions in the ⟨1 0 0⟩ diffraction pattern can now be understood in terms of the intersection of these ⟨1 1 1⟩ streaks with the sphere of reflection as illustrated schematically in Fig. 1d.

The existence of the microtwins was confirmed further by dark-field imaging. Fig. 2 shows a typical dark-field micrograph obtained by imaging a prominent satellite reflection, indicated by the arrow in Fig. 1c. This micrograph also reveals the boundary region between the completely amorphous area and the adjoining regions with the crystalline cover layer. A higher magnification image of the defects present near the interface in Fig. 2 showed small plate-like features in two distinct orientations. (See insert in Fig. 2). They are believed to be the microtwins responsible for the observed diffraction effects. As can be noticed, the microtwins are confined primarily to the region close to the amorphous–crystalline interface.

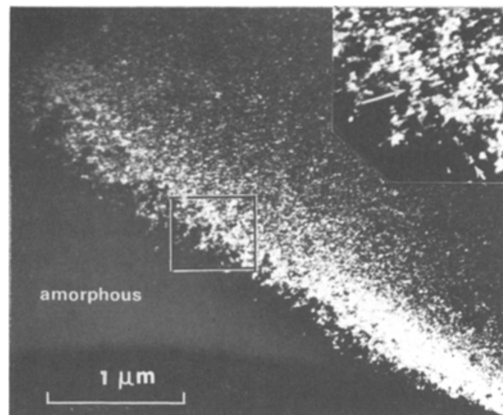

Figure 2 A dark-field micrograph obtained by imaging a twin reflection (indicated by the arrow in Fig. 1c) showing the presence of defects near the amorphous/ crystalline layer interface. Insert shows a high magnification image of microtwins.

A closer examination of the crystalline cover layer, which is approximately 2 μm thick, by preparing additional thin foil specimens showed that this region is characterized by a high density of "black dot defects". These are characteristic of radiation damage induced in crystalline material by high energy particles [7]. A typical example of this is shown in Fig. 3a, which is a bright-field micrograph obtained from the cover layer, removed from the amorphous crystalline interface. The crystalline nature of the cover layer is evident from the selected area electron diffraction pattern. The density of the "black dot defects" decreased somewhat with increase in distance from the interface. Fig. 3b shows a typical bright-field micrograph obtained from a region close to the implanted surface which reveals a smaller number of resolvable defects than in Fig. 3a. In addition to the small "black dots defects", the presence of several small prismatic dislocation loops having 300 to 400 Å diameter and exhibiting characteristic line of no-contrast perpendicular to the diffraction vector can also be noticed in this region (indicated by the arrows in Fig. 3b). The exact nature of these defects (namely vacancy or interstitial type) have not been unambiguously determined.

The type of crystal defects observed in the region immediately below the amorphous layer (namely in the crystalline substrate regions) was in general similar to those observed in the cover layer. However, in the regions removed from the

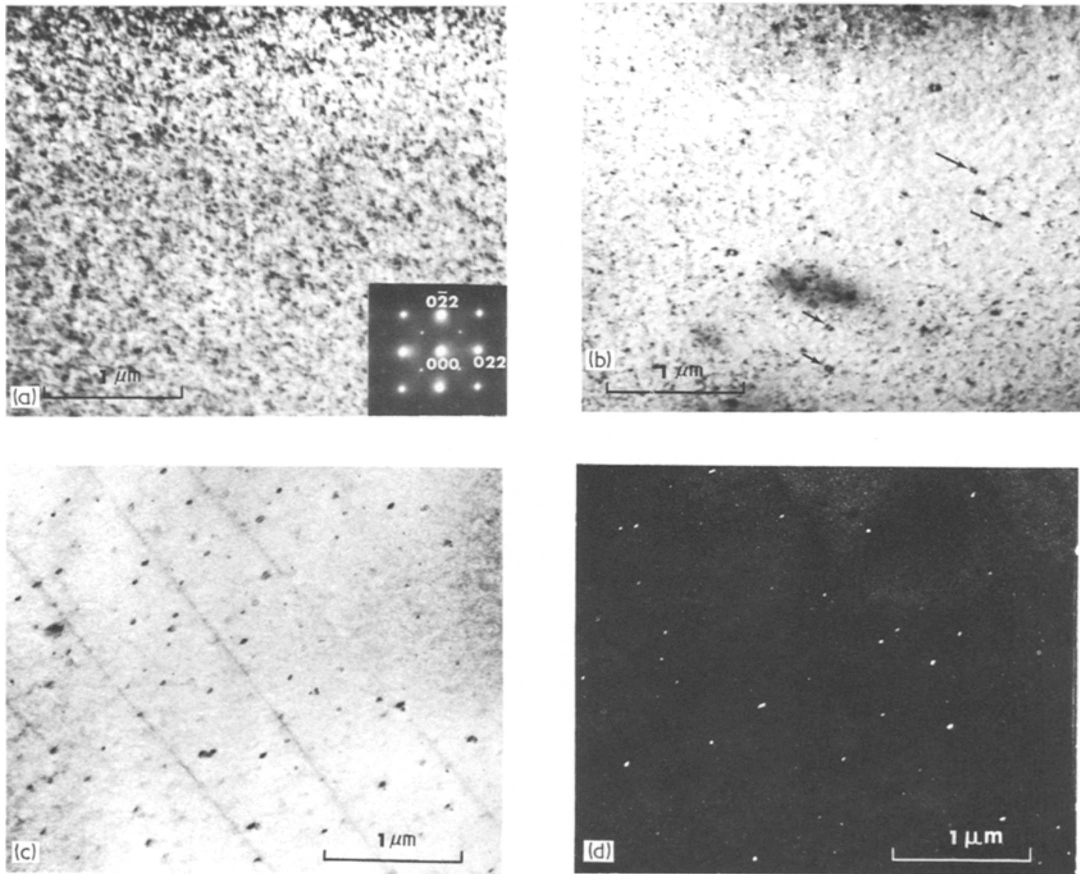

Figure 3 (a) Bright-field electron micrograph obtained from the crystalline cover layer region in the 2.7 MeV P^+ implanted GaAs specimen showing the distribution of lattice damage. The selected area electron diffraction pattern from this region is shown as an insert. (b) Bright-field micrograph obtained from a region closer to the surface than the one in Fig. 3a. Arrows indicate small prismatic dislocation loops. (c) Bright-field micrograph showing the presence of unidentified precipitates in the substrate regions below the amorphous layer. (d) Dark-field micrograph corresponding to the area in Fig. 3c.

substrate–amorphous layer interface the presence of thin plate-like or disk-shaped defects, which exhibited rather poor contrast could be noticed, as shown in Fig. 3c. These defects, although comparable in size to the loops observed in the cover layer, did not exhibit any dislocation loop contrast when imaged using several low order operating reflections. The dark-field images of these defects formed under the weak-beam conditions – a technique that enables small dislocation loops to be resolved as loops rather than as "black dots" – also failed to reveal any dislocation loop contrast (see Fig. 3d). In addition, dislocations which were present in the substrate near the interface were often found to be decorated with these unidentified particles. These observations suggest the possibility that the observed features are particles of a precipitating phase rather than small prismatic loops formed by point defect clustering. However, a positive identification of the exact nature of these precipitates could not be made owing to the absence of detectable effects in the selected area diffraction patterns.

Finally, under the conditions of high incident energies and heavy doses employed in the present studies, the specific ion used for implantation appears to play a relatively minor role in determining the nature and extent of the implantation induced damage in GaAs. The general conclusions regarding the lattice damage produced by the implantation of $^{31}P^+$ ions, have been found to be valid also in the case of GaAs specimens implanted with $^{14}N^+$ ions.

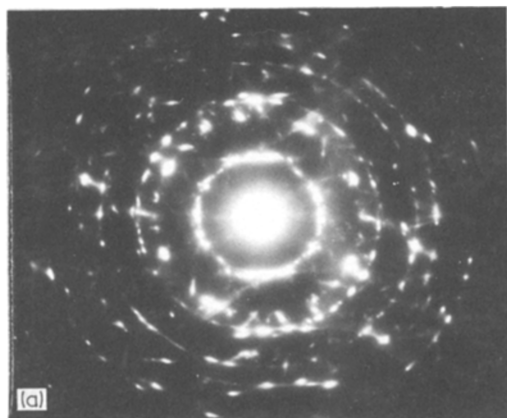

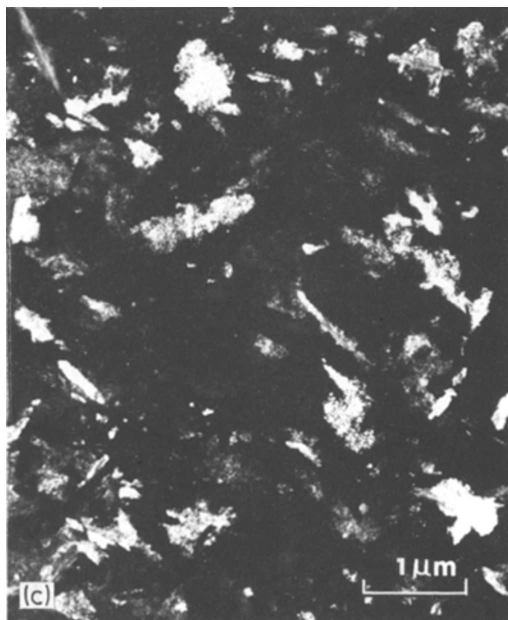

Figure 4 (a) Electron diffraction pattern from the implanted layer in a P^+ implanted specimen following annealing at 250° C for 6 h showing its fine-grained polycrystalline nature. (b) Bright-field micrograph corresponding to Fig. 4a showing the morphology of the recrystallized polycrystalline layer. (c) A dark-field micrograph obtained by imaging a segment of the bright diffraction ring in Fig. 4a showing shape of the individual crystallites.

3.2. Effects of post-implantation annealing

The recovery of the 2.7 MeV P^+ ion implantation induced lattice damage during post-implantation annealing treatments has been also followed by using electron microscopy. One set of samples was annealed at 250° C for 6 h while a second set was given an additional treatment at 400° C for 2 h in a two step annealing procedure. A third set of samples was annealed directly at 400° C for 4 h without the pre-treatment.

Fig. 4a shows a typical electron diffraction pattern obtained from the implanted layer following annealing at 250° C for 6 h. The pattern is composed of spotty rings, characteristic of a moderately fine grained polycrystalline structure. A closer examination of this diffraction pattern shows that rings corresponding to the reflections from the {2 0 0} {2 2 2} and {4 2 0} planes of the GaAs lattice are clearly absent and that distinct maxima occur on several of the rings that are present. The latter observations can be taken as an indication of the existence of some degree of preferred orientation of the recrystallized grains. Furthermore, it can be noticed that the spots on the rings in many cases are streaked along a particular direction and that a similar streak also appears at the origin (i.e. central spot). These streaks can be associated with the shape of individual crystallites, which can be best described as "thin plate-like" from the bright-field images (Fig. 4b). The exact size and shape of the individual crystallites can be better revealed by forming dark-field images of the intense diffraction spots appearing on the rings. Fig. 4c is a typical dark-field micrograph obtained from this specimen which shows the presence of thin plate-like crystallites having an irregular shape. Details of the defect structure within the individual crystallites could not be clearly resolved owing to the presence of a high density of residual defects in them.

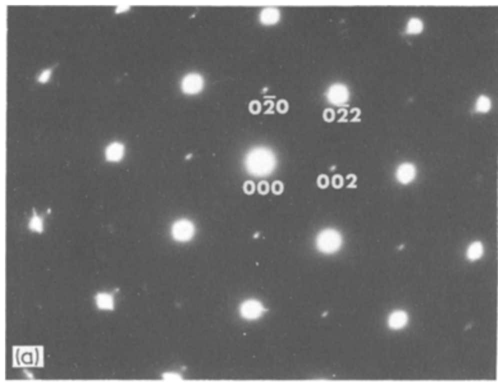

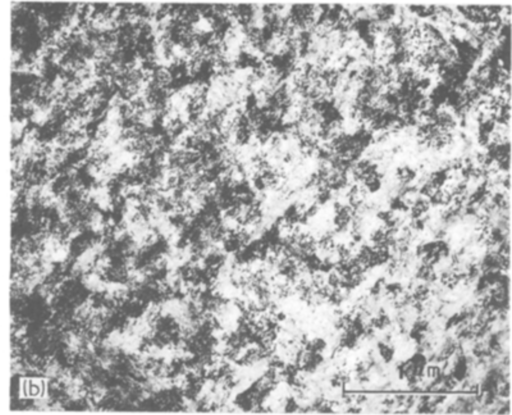

Figure 5 (a) Electron diffraction pattern from the P^+ implanted layer following the two stage annealing (namely 250° C for 6 h + 400° C for 2 h) showing the single crystalline nature of the regrown layer and its epitaxy with the ⟨1 0 0⟩ substrate. (b) Bright-field micrograph showing the morphological features of the regrown-layer.

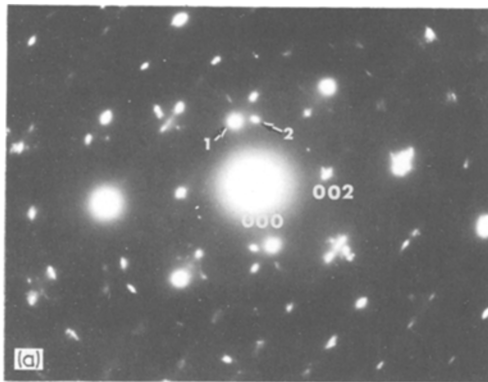

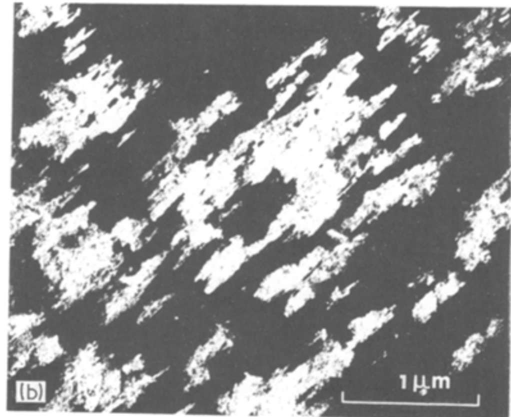

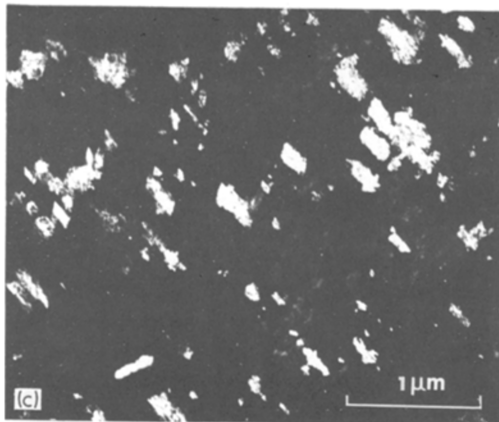

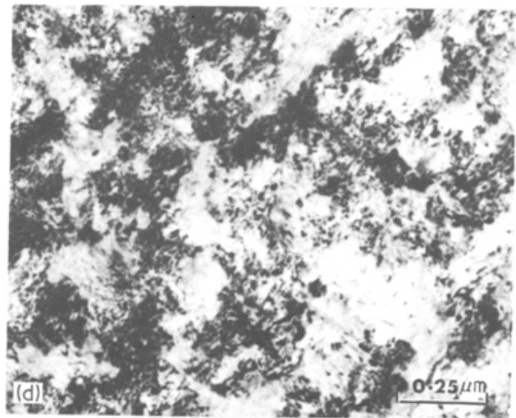

Figure 6 (a) Diffraction pattern obtained by tilting the specimen off the exact ⟨1 0 0⟩ orientation about the [0 0 2] axis showing the evolution of satellite reflections around the matrix reflections due to twinning on all {1 1 1} planes. (b) and (c) Dark-field micrographs obtained by imaging the twin reflections 1 and 2 respectively of Fig. 6a showing two different variants of the twin lamallae. (d) A high magnification bright-field micrograph showing the residual defects in the regrown layer.

The annealing at 250° C for 6 h was found to cause the recrystallization of both the buried amorphous and crystalline layers. The recrystallized polycrystalline layer, thus, extended from the original amorphous layer substrate interface to the surface, thereby eliminating the prior distinction between the cover and the buried layers.

The recrystallization of the amorphous layer in samples annealed directly at 400° C was also found to proceed by the growth of a polycrystalline layer having some degree of preferred orientation on the undamaged substrate. However, the samples which have been subjected to a two step annealing sequence, that is, annealing first at 250° C for 6 h followed by a second stage annealing at 400° C for 2 h, exhibited markedly different annealing behaviour. The electron diffraction patterns obtained form these samples (Fig. 5a) revealed that the recrystallized layer was essentially single crystal indicating that the regrowth of the damaged layer occurred epitaxially with the undamaged crystalline substrate. The bright-field micrographs of the regrown layer (Fig. 5b) showed that the morphology was drastically different from that observed after the first stage anneal and that the substructure was quite complex. In order to identify the nature of the substructure, further diffraction analysis was carried out. Tilting the specimen off the exact ⟨1 0 0⟩ orientation about a (0 0 2) axis was found to bring up additional satellite spots which were not in the (1 0 0) reciprocal lattice plane. This is illustrated in Fig. 6a which shows extra spots displaced from the original matrix reflections along the two perpendicular ⟨0 2 2⟩ directions. As was discussed in Section 3.1, the elongated elliptical shape of these satellite spots indicates that they arise from the intersections of the sphere of reflections with ⟨1 1 1⟩ streaks, and that these streaks probably arise from microtwins in the {1 1 1} orientations. This interpretation is further supported by the results of the dark-field analysis. Figs. 6b and c are two dark-field micrographs obtained by imaging the satellite reflections 1 and 2 (indicated by the arrows in Fig. 6a) respectively, which reveal the microtwins in two different {1 1 1} orientations.

In addition to the microtwins, other residual defects such as small prismatic dislocation loops and precipitates could be also observed in the microstructure. Fig. 6d is a high magnification bright-field micrograph revealing this feature. Owing to the complexity of the substructure a detailed analysis of the nature of these loops and precipitates was not carried out.

4. Discussion

4.1. Correlation of anneal stages with infra-red reflectivity measurements

It is interesting to compare the results of the present microstructural measurements with those of the previous infra-red studies in an attempt to determine the effect of the structural changes on the dielectric properties. The two studies are in reasonable agreement although the present results will modify one of the principal conclusions of the infra-red investigation. In the case of the as-implanted material, the present electron microscope studies have shown that the three-layer model for the implanted material proposed earlier by Kachare *et al.* is essentially correct. Implantation of 2.7 MeV $^{31}P^{+}$ ions at high doses, is shown to produce an amorphous layer, which is buried $\sim 2\ \mu m$ below the original surface of the sample. Since the diffraction pattern obtained from this layer shown in Fig. 1a indicates a reasonably well-defined ring structure, it can be inferred that the structure must still possess some degree of short range order. This is because for a truly amorphous structure, it should be virtually impossible to distinguish these rings from each other. The radii of the various rings observed in the diffraction pattern were measured accurately by carrying out optical densitometer traces across the diffraction pattern and the "*d*" spacing corresponding to each ring was calculated by using the camera contrast. The estimated values of interatomic spacings for the different rings are shown in Table I. The Bragg spacings corresponding to the three Debye rings show appreciable deviations from the "*d*" spacing for the crystalline material.

TABLE I A comparison of the estimated "*d*" spacings corresponding to the diffused rings in the diffraction pattern from amorphous GaAs with those for crystalline GaAs

	d spacings (Å)		
	Ring 1	Ring 2	Ring 3
Present work	3.30	1.91	1.25
Crystalline GaAs	3.264 (1 1 1)	1.999 (2 2 0)	1.154 (2 2 4)

Deviations of a similar nature have been reported also in the case of amorphous Si produced by ion implantation where it was shown that the amorphous material was 7% less dense than crystalline Si [8].

While no precise measurement of the extent of the buried layer was made, its position was found to correspond roughly with that deduced from the previous infra-red reflectivity measurements. The cover layer, which extends from the amorphous layer to the surface of the specimen was found to remain essentially crystalline, although this region was heavily damaged as characterized by the presence of a high density of "black dot defects." The crystalline substrate regions immediately below the amorphous buried layer, on the other hand, was shown to contain an unidentified precipitate phase.

The infra-red measurements of essentially identical non-annealed samples gave refractive indices for the cover and buried layers of 3.58 and 3.66, both substantially larger than the 3.30 value for the non-implanted GaAs. Assuming the crystalline cover-to-amorphous buried layer interface is thin compared to the infrared wavelength in the material, then the refractive index of heavily damaged but crystalline material near the interface is much closer to that of amorphous material than to the undamaged, crystalline value.

An interesting result that emerged from this investigation is the demonstration that the observed recovery and recrystallization of the damaged layer (namely cover and buried layers) proceeds during post-implantation annealing by different processes in the single step and two step annealing procedure. The first stage annealing at 250° C for 6 h was shown to result in the recrystallization of the amorphous and cover layers by random nucleation of feathery or thin plate-like grains producing a polycrystalline layer on the undamaged substrate. This process also eliminated the distinction between the cover and buried layers, and is similar to that envisaged by Kachare *et al.* [3] based on their infra-red reflectivity and X-ray diffraction analyses. The refractive indices of the cover and buried layers moved close to the non-implanted value of 3.30 after the recrystallization. This indicates that the damage level in the recrystallized polycrystalline material is much less than that in the as-implanted crystalline cover layer, at least in the region of high "black dot defect" density which should be influential in determining the apparent refractive index change at the crystalline–amorphous interface. Thus here also the two studies are in substantial agreement.

A major conclusion of the infra-red study was that there was no evidence for epitaxial recrystallization. However after subsequent annealing at 400° C the interference fringes were gone in one case and much reduced in another, and it was assumed that this was the result of further annealing of damage which remained after the 250° C anneal. It is now observed however, that an epitaxial recrystallization of the polycrystalline material takes place during the second stage annealing at 400° C through a regrowth of the implanted layer on the undamaged substrate. This latter recrystallization process is similar to that reported for high temperature annealing of heavily implanted silicon [4]. While the regrowth leads essentially to the formation of a single crystal, the regrown layer was found to contain a high density of microtwins and other types of lattice defects. Differences in the quality of the regrown materials could lead to differences in refractive indices and thus might explain the different results observed in the infra-red studies.

4.2. Comparison with previous studies involving lower energy–lower dose implantations

The low temperature annealing behaviour of the high energy, high dose P^+ implanted GaAs reported in the present study differs appreciably from that observed previously for GaAs implanted with other ions at lower energies and with somewhat lower doses but still sufficient to produce an amorphous layer. For example, Sealy [5] who studied the annealing behaviour of the continuous amorphous layer produced by the implantation of 1×10^{15} Te^+ ions cm^{-2} at 150 keV into ⟨1 1 0⟩ oriented GaAs substrates at room temperature, showed that the epitaxial recrystallization of disordered GaAs occurred upon annealing at 200 to 250° C. However, the investigations of Bicknell *et al.* [9] on GaAs implanted with 6×10^{14} Ar^+ ions cm^{-2} at 100 keV into ⟨1 0 0⟩ wafers revealed, that lattice re-ordering of the amorphous layer may occur upon annealing at temperatures as low as 120 to 150° C and lead to the formation of epitaxial layers. In another study, Mazey and Nelson [10] showed that epitaxial recrystalliza-

tion of the disordered layers in 60 keV Ne^+ implanted GaAs occurred upon annealing at temperatures in the range of 270 to 300° C. In contrast to these observations, the present study indicates that the recrystallization of the amorphous layer produced by the implantation of 2.7 MeV P^+ ions with a dose of $\sim 1 \times 10^{17}$ ions cm^{-2} both at 250° C and at 400° C does not proceed by the formation of an epitaxial single crystal layer but by the regrowth of a polycrystalline layer on the underlying substrate. Epitaxial regrowth was observed only after a two step annealing procedure where a specimen which was initially annealed at 250° C was subsequently annealed at 400° C. The present results, taken together with those of the previous investigations strongly suggest that the temperature range for epitaxial recrystallization may be dependent not only on the mass, the dose and the energy of the implanted ions, but also on the prior thermal history. It is interesting to note that similar differences have been observed in the recrystallization behaviour of amorphous Si produced by ion implantation. In particular, the investigations of Davidson and Booker [11] and of Matthews [12] showed that the thick amorphous layers produced by high dose ($> 6 \times 10^{14}$ ions cm^{-2}) implantation of Sb^+ ions into Si does not recrystallize epitaxially at temperatures up to 1000° C and the resulting material is partly polycrystalline. The amorphous layers produced by the implantation at lower doses or with lighter ions, however, recrystallize epitaxially at temperatures above $\sim 500°$ C. This behaviour has been attributed by some authors to the fact that high dose implantations often lead to dopant concentration levels exceeding solid solubility and upon annealing precipitation of a second phase may occur. These precipitates are believed to interfere with the epitaxial recrystallization giving rise to partially polycrystalline surfaces. Alternatively, the observations described above, lead one to believe that there may be "degree of amorphousness" in so far as epitaxial regrowth of the damped layer is concerned. When too much disorder is introduced, the driving force for homogeneous nucleation of recrystallized grains may become sufficiently large and cause random nucleation of grains within the amorphous layer away from the interface with the substrate where epitaxial regrowth is likely to initiate. This competition between random nucleation and epitaxial regrowth becomes particularly significant as the thickness of the amorphous layer is increased. In the single step annealing the dominance of the former leads to polycrystalline layers. In the two-step annealing procedure, where the recrystallized polycrystalline layer is subjected to a second stage anneal at a higher temperature, the grain growth kinetics dominates. At this stage the growth of the epitaxial layer from the substrate interface probably occurs by the migration of its boundary into the polycrystalline region, slowly consuming it. This is an energetically favourable process since it leads to considerable reduction in grain boundary area.

It is of interest to note that Csepregi *et al.* [13] have demonstrated a similar effect of thermal history on the epitaxial recrystallization of thick amorphous layers ($t > 2000$ Å) produced by high dose ion-implantation in Si. Their study showed that annealing of the amorphous layers produced by the implantation of 5×10^{14} As^+ ions cm^{-2} at 200 keV or 5×10^{15} B^+ ions cm^{-2} at 100 keV into ⟨1 1 1⟩ oriented Si at liquid nitrogen temperatures, directly at temperatures between 650 and 950° C leads to a highly disordered layer consisting of slightly misoriented grains and displaced atoms. However, specimens subjected to a two step annealing procedure, where the samples were first annealed at 550° C for periods as short as 1 h followed by a second stage anneal at 950° C for 30 min, showed almost complete recovery of the damage and epitaxial regrowth. The observations discussed here suggest that the annealing effects reported here may be found in many implanted semiconductors.

Acknowledgements

The research in part was sponsored by the Joint Services Electronics Program through Air Force Office of Scientific Research (AFSC) under contract F 44620-76-C-0061.

References

1. A. H. KACHARE, W. G. SPITZER, F. K. EULER and A. KAHAN, *J. Appl. Phys.* 45 (1974) 2938.
2. A. H. KACHARE, W. G. SPITZER and J. E. FREDRICKSON, *ibid.* 47 (1976) 4209.
3. A. H. KACHARE, W. G. SPITZER, J. E. FREDRICKSON and F. K. EULER, *ibid.* 47 (1976) 5374.
4. L. CSEPREGI, J. W. MAYER and T. W. SIGMON, *Phys. Lett.* A54 (1975) 157.

5. B. J. SEALY, *J. Mater. Sci.* 10 (1975) 683.
6. D. W. PASHLEY and M. J. STOWELL, *Phil. Mag.* 8 (1963) 1605.
7. M. RUHLE, M. WILKENS and V. ESSMANN, *Phys. Stat. Sol.* 11 (1965) 819.
8. D. J. MAZEY, R. S. NELSON and R. S. BARNES, *Phil. Mag.* 17 (1968) 1145.
9. R. BICKNELL, P. L. F. HEMMENT, E. C. BELL and J. E. TANSEY, *Phys. Stat. Sol. (a)* 12 (1972) K9.
10. D. J. MAZEY and R. S. NELSON, *Rad. Effects* 1 (1969) 229.
11. S. M. DAVIDSON and G. R. BOOKER, *ibid.* 6 (1970) 33.
12. M. D. MATTHEWS, *J. Mater. Sci.* 4 (1969) 997.
13. L. CSEPREGI, W. K. CHU, H. MULLER, J. W. MAYER and T. W. SIGMON, *Rad. Effects* 28 (1976) 227.

Received 19 September 1977 and accepted 18 April 1978.